PHYSICAL REVIEW C, VOLUME 63, 061301(R)

Lifetimes of superdeformed rotational states in ^{36}Ar

C. E. Svensson,[1,2] A. O. Macchiavelli,[1] A. Juodagalvis,[3,*] A. Poves,[4] I. Ragnarsson,[3] S. Åberg,[3] D. E. Appelbe,[5,†] R. A. E. Austin,[5] G. C. Ball,[6] M. P. Carpenter,[7] E. Caurier,[8] R. M. Clark,[1] M. Cromaz,[1] M. A. Deleplanque,[1] R. M. Diamond,[1] P. Fallon,[1] R. V. F. Janssens,[7] G. J. Lane,[1] I. Y. Lee,[1] F. Nowacki,[9] D. G. Sarantites,[10] F. S. Stephens,[1] K. Vetter,[1] and D. Ward[1]

[1]*Nuclear Science Division, Lawrence Berkeley National Laboratory, Berkeley, California 94720*
[2]*Department of Physics, University of Guelph, Guelph, Ontario, Canada N1G 2W1*
[3]*Department of Mathematical Physics, Lund Institute of Technology, S-22100 Lund, Sweden*
[4]*Departamento de Física Teórica, Universidad Autónoma de Madrid, E-28049 Madrid, Spain*
[5]*Department of Physics and Astronomy, McMaster University, Hamilton, Ontario, Canada L8S 4M1*
[6]*TRIUMF, 4004 Wesbrook Mall, Vancouver, British Columbia, Canada V6T 2A3*
[7]*Argonne National Laboratory, Argonne, Illinois 60439*
[8]*Institut de Recherches Subatomiques, IN2P3-CNRS-Université Louis Pasteur, F-67037 Strasbourg Cedex 2, France*
[9]*Laboratoire de Physique Theorique, Université Louis Pasteur, F-67084 Strasbourg Cedex, France*
[10]*Chemistry Department, Washington University, St. Louis, Missouri 63130*

(Received 27 October 2000; published 1 May 2001)

Lifetimes have been measured in a superdeformed rotational band recently identified in the $N=Z$ nucleus ^{36}Ar. A large low-spin quadrupole deformation ($\beta_2=0.46\pm0.03$) is confirmed and a decrease in the collectivity is observed as the high-spin band termination at $I^{\pi}=16^{+}$ is approached. Detailed comparisons of the experimental $B(E2)$ values with the results of cranked Nilsson-Strutinsky and large-scale $(s_{1/2}d_{3/2})$-pf spherical shell model calculations indicate the need for a more refined treatment of transition matrix elements close to termination in the former, and the inclusion of the complete sd-pf model space in the latter description of this highly-collective rotational band.

DOI: 10.1103/PhysRevC.63.061301 PACS number(s): 21.10.Re, 21.10.Tg, 23.20.Lv, 27.30.+t

The microscopic description of collective motion in the many-nucleon system is a fundamental goal of nuclear structure physics. Progress in this direction is closely linked with the identification of the symmetries governing the underlying many-particle dynamics. In the lower sd-shell nuclei, the degeneracies of the harmonic oscillator potential remain approximately valid and the resulting SU(3) symmetry plays a central role in understanding the relationship between the deformed intrinsic states of rotors such as ^{20}Ne and ^{24}Mg, and the laboratory-frame shell-model description of these nuclei [1]. In heavier nuclei, the strong spin-orbit interaction destroys the oscillator SU(3) symmetry, and a direct shell-model approach to rotational motion is also rendered impractical by the huge dimensionalities of the valence spaces. Considerable effort has thus been devoted to the identification of approximate symmetries which enable a microscopic description of rotational motion in these nuclei within an appropriately truncated model space (cf. [2–4]). It is important to test the validity of such models with experimental data and exact diagonalizations in cases where the valence space is large enough for collective rotation to develop, yet small enough to be approached from the shell-model perspective. Detailed experimental [5–7] and theoretical [8–13] studies of the deformed pf-shell rotor ^{48}Cr have led to considerable progress in this direction. The recent identification of a superdeformed (SD) band in ^{36}Ar [14], in which four particles are promoted from the sd to the pf shell, permits an extension of these studies to a case where, in analogy with rotational motion in heavier nuclei, two major shells are active for both protons and neutrons. In this Rapid Communication, we report lifetime measurements which provide sensitive tests of the theoretical description of this highly-collective rotational band.

High-spin states in ^{36}Ar were populated via the ^{24}Mg(^{20}Ne,2α)^{36}Ar reaction in two experiments. In the first, the target consisted of a self-supporting 440 μg/cm^2 foil of ^{24}Mg, while in the second the 420 μg/cm^2 ^{24}Mg target was backed by 11.75 mg/cm^2 of Au, sufficient to stop all of the recoiling nuclei. In each case, an 80-MeV ^{20}Ne beam of $\sim$2 pnA intensity was provided by the ATLAS facility at Argonne National Laboratory. Gamma-rays were detected with 101 HPGe detectors of the GAMMASPHERE array [15], arranged in 16 annular rings at angles between 31.7° and 162.7° relative to the beam axis. The Hevimet collimators were removed from the HPGe detectors to enable event-by-event γ-ray multiplicity and sum-energy measurements [16] and evaporated charged particles were detected with the Microball [17], a 4π array of 95 CsI(Tl) scintillators. Events populating ^{36}Ar were cleanly selected by requiring the detection of two α particles in combination with a total detected γ-ray plus charged-particle energy consistent with the Q value for the 2α channel [18]. Totals of 7.75×10^8 and 8.27×10^8 γ-γ-γ and higher-fold coincidence events were recorded in the first and second experiments, respectively.

*Present addresses: Physics Division, Oak Ridge National Laboratory, Oak Ridge, TN 37831-6373 and Department of Physics and Astronomy, University of Tennessee, Knoxville, TN 37996-1200.

†Present address: Daresbury Laboratory, Daresbury, Warrington WA4 4AD, U.K.

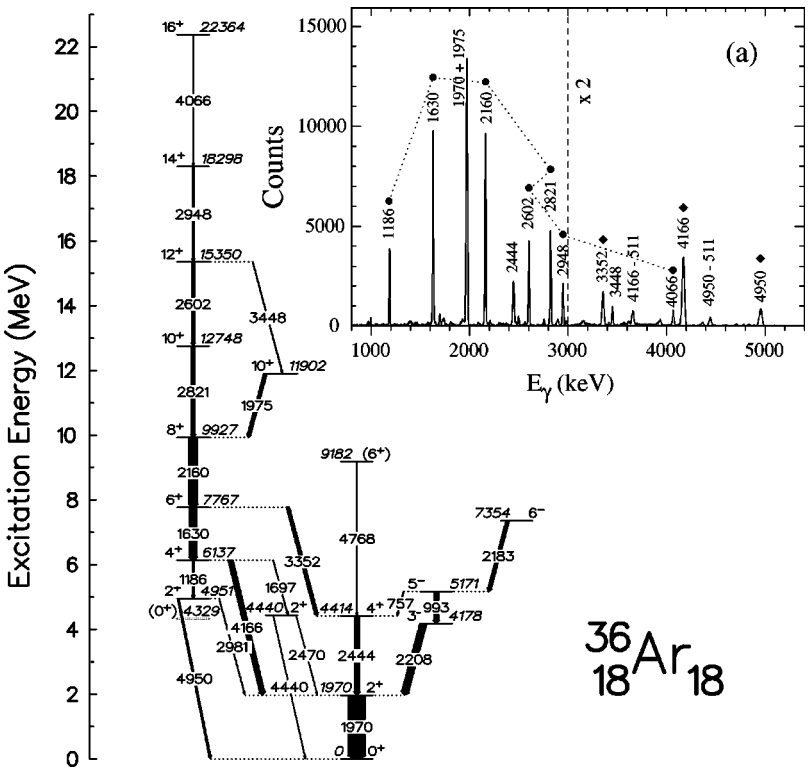

FIG. 1. Partial decay scheme for ^{36}Ar showing the superdeformed band at the left. Level and γ-ray energies are given to the nearest keV and the arrow widths are proportional to transition intensities. The inset shows the γ-ray spectrum obtained by summing coincidence gates set on all members of the SD band (circles). Diamonds indicate linking transitions connecting the band to low-spin states in ^{36}Ar. For clarity, the spectrum has been multiplied by 2 for $E_\gamma \geqslant 3$ MeV.

A partial decay scheme for ^{36}Ar, showing states relevant to the present discussion, is presented in Fig. 1. The inset shows the γ-ray spectrum from the thin target experiment obtained by summing coincidence gates set on all members of the SD band. Configuration-dependent [19] cranked Nilsson-Strutinsky (CNS) calculations and large-scale $(s_{1/2}d_{3/2})$-pf shell-model (SM) diagonalizations with the ANTOINE code [20] assign the band to a configuration in which four pf-shell orbitals are occupied. A comparison of these calculations with the energetic properties of the band was presented in Ref. [14]. Here we focus on tests of the predicted electromagnetic properties based on state lifetime measurements.

Equilibrium deformations in the (ε_2, γ) plane from the CNS calculations are shown in Fig. 2. At low spin, a prolate deformation $\varepsilon_2 = 0.40$ ($\beta_2 \approx 0.45$), which remains approximately constant up to $I = 8\hbar$, is calculated. At higher spins the nucleus is predicted to change shape smoothly, with the band terminating at $I^\pi = 16^+$ in a fully-aligned oblate ($\gamma = 60°$) state. Assuming the rotor model and the initial-state deformations, the $B(E2)$ values corresponding to this shape trajectory are shown by the circles in Fig. 2(a). At low spin, the predicted excursion to negative γ values leads to $B(E2)$'s slightly larger than those of an $\varepsilon_2 = 0.40$ prolate rotor, while at high spin the transition to an oblate shape implies a loss of collectivity and a vanishing $B(E2)$ at the terminating state. Also shown in Fig. 2(a) are the $B(E2)$ values from the shell-model calculations, with the effects of core polarization associated with $2\hbar\omega$ excitations outside of the model space accounted for by use of the isoscalar effective charges $q_\pi = 1.5$ and $q_\nu = 0.5$. The spin dependence is observed to be weaker in the SM than in the CNS calculations, with the SM $B(E2)$ values remaining substantial as the band termination is approached.

In order to test the quadrupole properties predicted by the two models, we have measured state lifetimes throughout the ^{36}Ar band by Doppler-shift attenuation techniques. For the high-spin states ($I \geqslant 8\hbar$), the high transition energies lead to lifetimes which are short compared to the mean time ($\sim$100 fs) taken by the recoils to exit the ^{24}Mg target. These lifetimes were measured by the thin-target centroid-shift method [21]. For each transition from an SD state, the centroid of the γ-ray peak was measured in spectra from each of the 16 rings of the GAMMASPHERE array. These data were fitted to obtain the mean Doppler shift associated with each transition. The resulting fractions F of the full Doppler shift

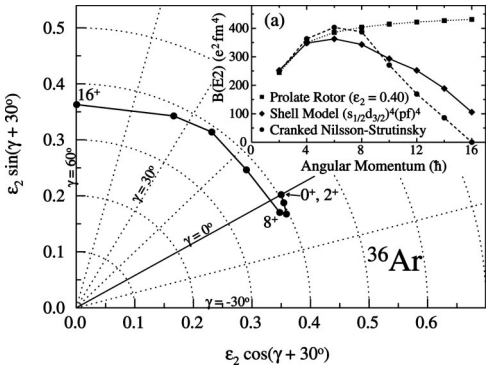

FIG. 2. Calculated shape trajectory in the (ε_2, γ) plane for the SD band in ^{36}Ar. The inset (a) shows the predicted $B(E2; I \rightarrow I-2)$ values from the shell model (diamonds) and cranked Nilsson-Strutinsky (circles) calculations. The $B(E2)$'s for a fixed prolate deformation $\varepsilon_2 = 0.40$ are also shown for comparison (squares).

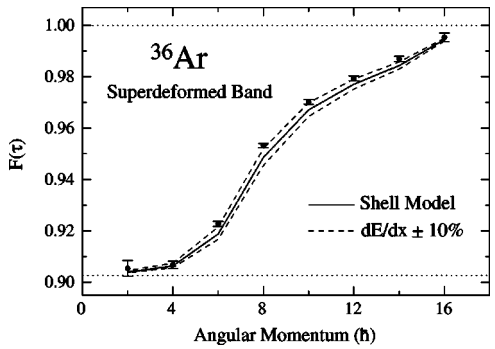

FIG. 3. Fractional Doppler shifts F measured for transitions in the ^{36}Ar superdeformed band in the thin-target experiment. The solid line shows the F values calculated using the shell-model $B(E2)$'s and SRIM-2000 stopping powers. The corresponding values obtained by scaling the stopping powers by $\pm 10\%$ are shown by the dashed lines. The dotted lines at $F=1.00$ and $F=0.903$ represent the full Doppler shift and the mean value for recoils which have exited the thin-target.

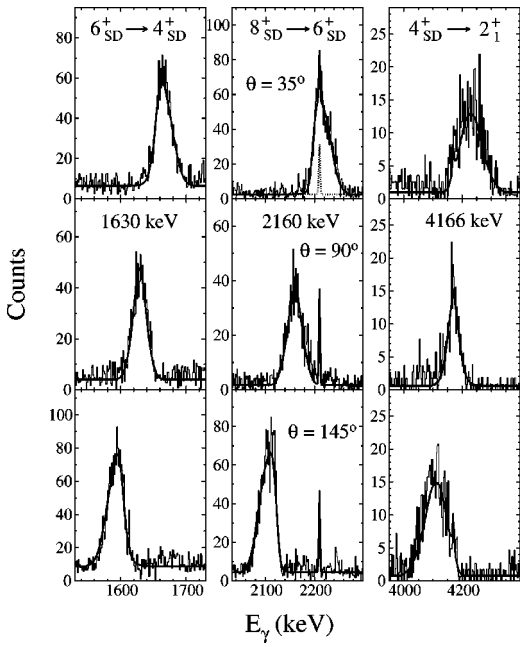

FIG. 4. Doppler-shift attenuation lineshape analyses from the backed-target experiment. The left, middle, and right columns present data for the 1630, 2160, and 4166 keV transitions, respectively, while the top, middle, and bottom rows correspond to mean angles of 35°, 90°, and 145° relative to the beam axis. The fully-stopped peak in the middle column is the 2208 keV $3^-_1 \rightarrow 2^+_1$ transition in ^{36}Ar and arises from coincidence with a weak 2604 keV γ ray (not shown in Fig. 1) contaminating the 2602 keV gating transition.

are shown in Fig. 3. In cases where more than one decay branch was observed from a given state, the weighted average F value is presented. With the exception of the 4066 keV γ ray from the terminating state, these Doppler shifts were measured with gates set on in-band transitions above the γ ray of interest. The time structures of the feeding associated with the actual gating transitions used in the analysis were incorporated in the fitting procedure, which began at the top of the band and allowed a variable lifetime value for each state. Stopping powers were calculated with the SRIM-2000 code [22]. Also shown in Fig. 3 are the F values (solid line) calculated assuming the shell-model $B(E2)$ values. These calculations clearly underestimate the measured Doppler shifts at intermediate spins, indicating that the SM $B(E2)$'s are smaller than the experimental values and/or that the stopping powers used in the calculation were too large. In order to investigate sensitivity to the stopping powers, the calculations were repeated with the SRIM-2000 values shifted by $\pm 10\%$, a generous estimate of their uncertainty. As shown by the dashed lines in Fig. 3, even at the lower extreme of this range the F values calculated with the SM $B(E2)$'s remain systematically below the measured values for the intermediate-spin states.

For the lower-spin states in the ^{36}Ar SD band, a substantial fraction of the decays take place after the recoils have exited the ^{24}Mg target. For these states, additional lifetime information was obtained in the backed-target experiment. Figure 4 shows examples of γ-ray lineshapes for transitions from the 8^+, 6^+, and 4^+ SD states. These spectra were obtained by gating on the 2821 and 2602 keV transitions, which defined the feeding time structure and eliminated the slow feeding component from the 11902-keV, 10^+ state. The spectra at mean angles of 35°, 90°, and 145° relative to the beam axis were simultaneously fitted using a version of the LINESHAPE code [23] modified so that the initial ^{36}Ar recoil momenta used in the stopping simulations were sampled from the experimental distribution calculated from the momenta of the α particles detected in the Microball. This procedure, which correctly accounts for both the broad initial recoil momentum distribution produced by the α-particle evaporation and the bias in this distribution resulting from the angle-dependent particle detection efficiency, was essential to obtain the excellent fits to the lineshapes illustrated in Fig. 4. Equally good fits were obtained with the three stopping power options available in the code, with the deduced mean lifetimes varying by less than $\pm 5\%$. In order to match the procedure for the thin-target measurements discussed above, we have adopted the Ziegler and Chu [24] stopping powers and assigned a conservative $\pm 10\%$ uncertainty.

Lifetime and $B(E2)$ values for all transitions involving members of the SD band, from both the thin- and backed-target experiments, are summarized in Table I. We note that the $B(E2)$ of $372 \pm 59\ e^2\ \mathrm{fm}^4$ for the $4^+ \rightarrow 2^+$ SD transition corresponds to a deformation $\beta_2 = 0.46 \pm 0.03$ for a prolate shape. The $B(E2)$'s for the in-band transitions are compared with the CNS and SM calculations in Fig. 5. The inner error bars in this figure represent the statistical uncertainties, while the outer error bars show the effects of $\pm 10\%$ shifts in the stopping powers. For the terminating state, the necessity of gating from below leaves the possibility of a feeding delay and yields only an upper limit on the state lifetime. Nevertheless, the lower limit of $84\ e^2\ \mathrm{fm}^4$ derived for the $16^+ \rightarrow 14^+$ $B(E2)$ corresponds to 12 Weisskopf units (W.u.), confirming the shell-model prediction of a substantial remaining collectivity. The CNS calculations are in quite good agreement with the experimental $B(E2)$ values at low spin,

TABLE I. Spins, γ-ray energies, branching ratios, mean lifetimes, and $B(E2;I\rightarrow I-2)$ values for transitions involving SD states (subscript S) in ^{36}Ar. The uncertainties for the lifetime and $B(E2)$ values include both the statistical uncertainties and the effects of an estimated $\pm 10\%$ uncertainty in the stopping powers. The lifetime of the 8^+ state is a weighted average from the thin- and backed-target measurements.

I_i^π	I_f^π	E_γ (keV)	B (%)	τ (fs)	$B(E2)$ (e^2 fm^4)
2_S^+	0_S^+	622	<0.8	48(24)	
4_S^+	2_S^+	1186.0(3)	20.3(8)	190(30)	372(59)
6_S^+	4_S^+	1629.8(3)	70.0(12)	109(16)	454(67)
8_S^+	6_S^+	2160.0(3)	100	39.5(62)	440(70)
10_S^+	8_S^+	2821.4(4)	100	14.5(33)	316(72)
12_S^+	10_S^+	2602.2(4)	81.7(12)	20.3(41)	275(56)
14_S^+	12_S^+	2947.7(5)	100	15.8(36)	232(53)
16_S^+	14_S^+	4066.4(12)	100	<8.7	>84
2_S^+	0_1^+	4949.8(16)	79.3(14)	48(24)	4.6(23)
4_S^+	2_1^+	4165.6(10)	73.4(9)	190(30)	2.5(4)
4_S^+	2_2^+	1696.7(4)	6.3(4)	190(30)	19.2(30)
6_S^+	4_1^+	3352.5(8)	30.0(12)	109(16)	5.3(8)
10_1^+	8_S^+	1974.8(10)	100	623(106)	43.6(74)
12_S^+	10_1^+	3448.4(10)	18.3(12)	20.3(41)	15.0(30)

but underestimate the high-spin collectivity. These results are not unexpected. Although pairing correlations are neglected in the CNS calculations, these correlations lead to only a minor perturbation of the wave function for such strongly deformed bands [9,11], and the low-spin quadrupole properties are thus accurately reproduced. At high spin, quantum fluctuations about the equilibrium deformations of Fig. 2 are expected to become relatively more important as the rotational $B(E2)$ values decrease. In Ref. [13], inclusion of the zero-point motion in the ε_2 direction was shown to lead to excellent agreement between the CNS and SM $B(E2)$ values for ^{48}Cr. For the ^{36}Ar SD band, shape fluctuations in the γ degree of freedom will also be important,

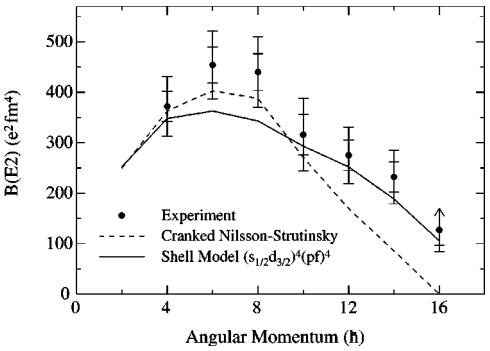

FIG. 5. $B(E2;I\rightarrow I-2)$ values for the SD band in ^{36}Ar compared with the results of cranked Nilsson-Strutinsky (dashed line) and $(s_{1/2}d_{3/2})^4(pf)^4$ shell model (solid line) calculations. The inner error bars represent statistical uncertainties, while the outer error bars show the effects of systematic $\pm 10\%$ shifts in the stopping powers (see text for details).

particularly in removing the artificial vanishing of the CNS transition matrix element at the terminating state where the mean field predicts an oblate ($\gamma=60°$) equilibrium deformation.

As shown in Fig. 5, the SM calculations provide a good description of the spin-dependence of the $B(E2)$'s, but systematically underestimate the absolute values, particularly for the 6^+ and 8^+ SD states. An excellent fit to the data ($\chi^2/\nu=0.84$) is obtained by simply scaling all of the SM $B(E2)$ values by a factor of 1.20. While this result could, in principle, be achieved by increasing the effective charges, the isoscalar values employed here accurately describe $B(E2)$ values in calculations for other $N=Z$ nuclei (cf. Ref. [7]), and are expected to be equally appropriate for ^{36}Ar in a ''complete'' valence space. In this context, we note that the CNS calculations predict that the spherical $d_{5/2}$ orbital is only $\sim 90\%$ full in the ^{36}Ar SD band, while dimensionality considerations required this orbital to be closed in the SM calculations. The impressive description of the energetic properties of the band [14] by the SM calculations indicates that the influence of such $d_{5/2}$ holes on the moment of inertia has been effectively subsumed in the 1 MeV lowering of the $s_{1/2}$ energy necessary to reproduce the ^{29}Si spectrum in the truncated space. However, this provides no guarantee that the $d_{5/2}$-hole contribution to the quadrupole moment has been properly accounted for. The intrinsic quadrupole moment $Q_0=113\ e$ fm^2 obtained in the $(s_{1/2}d_{3/2})^4(pf)^4$ model space, from either the low-spin spectroscopic quadrupole moments or the calculated in-band $B(E2;2^+\rightarrow 0^+)$ value, already represents 80% of the maximum available in the full $(sd)^{16}(pf)^4$ space (as realized in the SU(3) limit [27,28]). Nevertheless, a $\sim 5-10\,\%$ increase in the quadrupole moment, corresponding to a 10–20 % increase in the $B(E2)$'s, from the $d_{5/2}$-hole component in the wave function is plausible, and would considerably improve the agreement with experiment. Indeed, projected shell model [25] calculations including the entire $N=1$, 2, and 3 major shells have recently been performed for the ^{36}Ar SD band [26]. These calculations, using the same isoscalar effective charges employed here, yield $B(E2)$ values which are 10–20 % larger than those of the $(s_{1/2}d_{3/2})^4(pf)^4$ SM calculation, in good agreement with the experimental data presented in Fig. 5.

Further study of the role of the $d_{5/2}$ orbital in the ^{36}Ar SD band, perhaps through a complete sd-pf diagonalization by quantum Monte Carlo techniques [29] would be of considerable interest. Such a calculation would also provide insight into the mixing of configurations involving different numbers of excitations across the $N,Z=20$ shell gap. Such mixing is important for an understanding of the interaction of the 10^+ SD state with the nearby yrast 10^+ state at 11902 keV [predicted to belong to the dominantly $(pf)^2$ configuration in both calculations], and also the decay out of the band at low spin. For the latter, we note that the $B(E2)$ values given in Table I for the $4p$-$4h$ transitions connecting the 2^+, 4^+, and 6^+ SD states to the ground band are in the range of 0.3–0.8 W.u. These are comparable to the decay-out transition strengths measured for the SD band in ^{60}Zn [30], which involves the analogous $4p$-$4h$ excitation across the

$N,Z=28$ shell gap, but are 3–4 orders of magnitude larger than an upper limit set on the $E2$ decay-out strength in ^{194}Pb [31]. In the heavier nuclei, the superdeformed to spherical transition involves the rearrangement of a large number of particles. Nevertheless, the opportunity to study the microscopic structure of the wave function components which contribute to the decay-out transitions in ^{36}Ar could provide new insight into the macroscopic barrier-penetration models [32] which have been used to describe this process.

In summary, lifetimes have been measured throughout a superdeformed band recently identified in ^{36}Ar. The low-spin $B(E2)$ values, corresponding to $\beta_2=0.46\pm0.03$ for a prolate shape, are in agreement with cranked Nilsson-Strutinsky calculations, but suggest the need to include the complete sd-pf space in the shell-model description of this highly collective rotational band. At high spin, the $B(E2)$ values decrease, but remain significant ($\geqslant$12 W.u.) at the terminating 16^+ state, in agreement with the SM predictions. With essentially complete spectroscopic information, including spins, parities, excitation energies, and $B(E2)$ values, combined with a valence space small enough to be approached from the shell model perspective, the ^{36}Ar superdeformed band provides many exciting opportunities for further studies of the microscopic structure of collective motion in nuclei.

This work has been partially supported by the U.S. DOE under Contract Nos. DE-AC03-76SF00098, W-31-109-ENG-38, and DE-FG05-88ER40406, the Natural Sciences and Engineering Research Council of Canada, the Swedish Institute, NFR (Sweden), DGES (Spain) under Grant No. PB96-53, and IN2P3 (France).

[1] J.P. Elliott, Proc. R. Soc. London, Ser. A **245**, 128 (1958); **245**, 562 (1958).
[2] A.P. Zuker, J. Retamosa, A. Poves, and E. Caurier, Phys. Rev. C **52**, R1741 (1995).
[3] C. Vargas, J.G. Hirsch, T. Beuschel, and J.P. Draayer, Phys. Rev. C **61**, 031301(R) (2000).
[4] C. Bahri and D.J. Rowe, Nucl. Phys. **A662**, 125 (2000).
[5] J.A. Cameron *et al.*, Phys. Lett. B **387**, 266 (1996).
[6] S.M. Lenzi *et al.*, Z. Phys. A **354**, 117 (1996).
[7] F. Brandolini *et al.*, Nucl. Phys. **A642**, 387 (1998).
[8] E. Caurier, A.P. Zuker, A. Poves, and G. Martínez-Pinedo, Phys. Rev. C **50**, 225 (1994).
[9] E. Caurier *et al.*, Phys. Rev. Lett. **75**, 2466 (1995).
[10] A. Juodagalvis and S. Åberg, Phys. Lett. B **428**, 227 (1998).
[11] A. Poves, J. Phys. G **25**, 589 (1999).
[12] K. Hara, Y. Sun, and T. Mizusaki, Phys. Rev. Lett. **83**, 1922 (1999).
[13] A. Juodagalvis, I. Ragnarsson, and S. Åberg, Phys. Lett. B **477**, 66 (2000).
[14] C.E. Svensson *et al.*, Phys. Rev. Lett. **85**, 2693 (2000).
[15] I.-Y. Lee, Nucl. Phys. **A520**, 641c (1990).
[16] M. Devlin *et al.*, Nucl. Instrum. Methods Phys. Res. A **383**, 506 (1996).
[17] D.G. Sarantites *et al.*, Nucl. Instrum. Methods Phys. Res. A **381**, 418 (1996).
[18] C.E. Svensson *et al.*, Nucl. Instrum. Methods Phys. Res. A **396**, 228 (1997).
[19] T. Bengtsson and I. Ragnarsson, Nucl. Phys. **A436**, 14 (1985); A.V. Afanasjev and I. Ragnarsson, *ibid.* **A591**, 387 (1995).
[20] E. Caurier, computer code ANTOINE, Strasbourg, 1989.
[21] B. Cederwall *et al.*, Nucl. Instrum. Methods Phys. Res. A **354**, 591 (1995).
[22] J.F. Ziegler, http://www.research.ibm.com/ionbeams
[23] J.C. Wells *et al.*, Report ORNL-6689, 1991.
[24] J.F. Ziegler and W.K. Chu, At. Data Nucl. Data Tables **13**, 463 (1974).
[25] K. Hara and Y. Sun, Int. J. Mod. Phys. E **4**, 637 (1995).
[26] G.-L. Long and Y. Sun, Phys. Rev. C **63**, 021305(R) (2001).
[27] It has been shown (cf. [28]) that in well-deformed rotational bands the mixing of SU(3) representations produced by the spin-orbit and pairing interactions can be coherent, i.e., spin independent, leaving SU(3) as a ''quasidynamical'' symmetry and the *relative* $B(E2)$'s close to their SU(3) values. For ^{36}Ar, the near saturation of the *absolute* SU(3) $B(E2)$ values suggests that the wave functions for the low-spin members of the SD band are both highly coherent and, despite the large spin-orbit splitting in both the sd and pf shells, dominated by a relatively small number of the leading SU(3) representations.
[28] P. Rochford and D.J. Rowe, Phys. Lett. B **210**, 5 (1988); D.J. Rowe, C. Bahri, and W. Wijesundera, Phys. Rev. Lett. **80**, 4394 (1998); C. Bahri, D.J. Rowe, and W. Wijesundera, Phys. Rev. C **58**, 1539 (1998); V.G. Gueorguiev, J.P. Draayer, and C.W. Johnson, *ibid.* **63**, 014318 (2001).
[29] M. Honma, T. Mizusaki, and T. Otsuka, Phys. Rev. Lett. **77**, 3315 (1996); T. Otsuka, M. Honma, and T. Mizusaki, *ibid.* **81**, 1588 (1998).
[30] C.E. Svensson *et al.*, Phys. Rev. Lett. **82**, 3400 (1999).
[31] R. Krücken *et al.*, Phys. Rev. C **55**, R1625 (1997).
[32] E. Vigezzi, R.A. Broglia, and T. Døssing, Phys. Lett. B **249**, 163 (1990), Nucl. Phys. **A520**, 179c (1990); Y.R. Shimizu *et al.*, *ibid.* **A557**, 99c (1993).